Silicon-tethered colchicine aryne cyclo-adduct as a potent molecule for the abrogation of epithelial to mesenchymal transition *via* modulating cell cycle regulatory CDK-2 and CDK-4 kinases

Waseem Iqbal Lone[a,b,1], Jagdish Chand[b,1], Puneet Kumar,[a,b] Zabeer Ahmed[b,c], Debaraj Mukherjee,[a,d] Anindya Goswami[2,3*], Jasha Momo H. Anal[1,3*]

[a]Natural Products and Medicinal Chemistry Division, CSIR– Indian Institute of Integrative Medicine, Jammu-180001, India.

[b]Pharmacology Division, CSIR– Indian Institute of Integrative Medicine, Jammu-180001, India.

[c]Academy of Scientific and Innovative Research (AcSIR), Ghaziabad - 201002, India

[d]Department of Chemical Sciences, Bose Institute, EN-80, Sector V, Kolkata-700091, WB, India

[1]Authors contributed equally to this work.

***Corresponding authors**:
Jasha Momo H. Anãl, PhD.
Scientist, Natural Products and Medicinal Chemistry Division,
CSIR-Indian Institute of Integrative Medicine, Jammu-180001, India.
E-mail: hmunshel.jasha@iiim.res.in /agoswami@iiim.ac.in

https://doi.org/10.26434/chemrxiv-2024-rs3lh **ORCID:** https://orcid.org/0000-0003-2378-3944 Content not peer-reviewed by ChemRxiv. **License:** CC BY-NC-ND 4.0

Highlights

- Regioselective Cycloaddition on colchicine with arynes lead to the synthesis of various colchicine derivatives.
- Endo-facial cycloaddition occurs preferentially on the tropolone moiety of colchicine.
- Silicon-conjugated derivative of colchicine **B-4a** was found to be most potent against breast cancer and abrogated cell cycle regulatory kinases (cdk-2 and cdk-4) activity.

Graphical Abstract

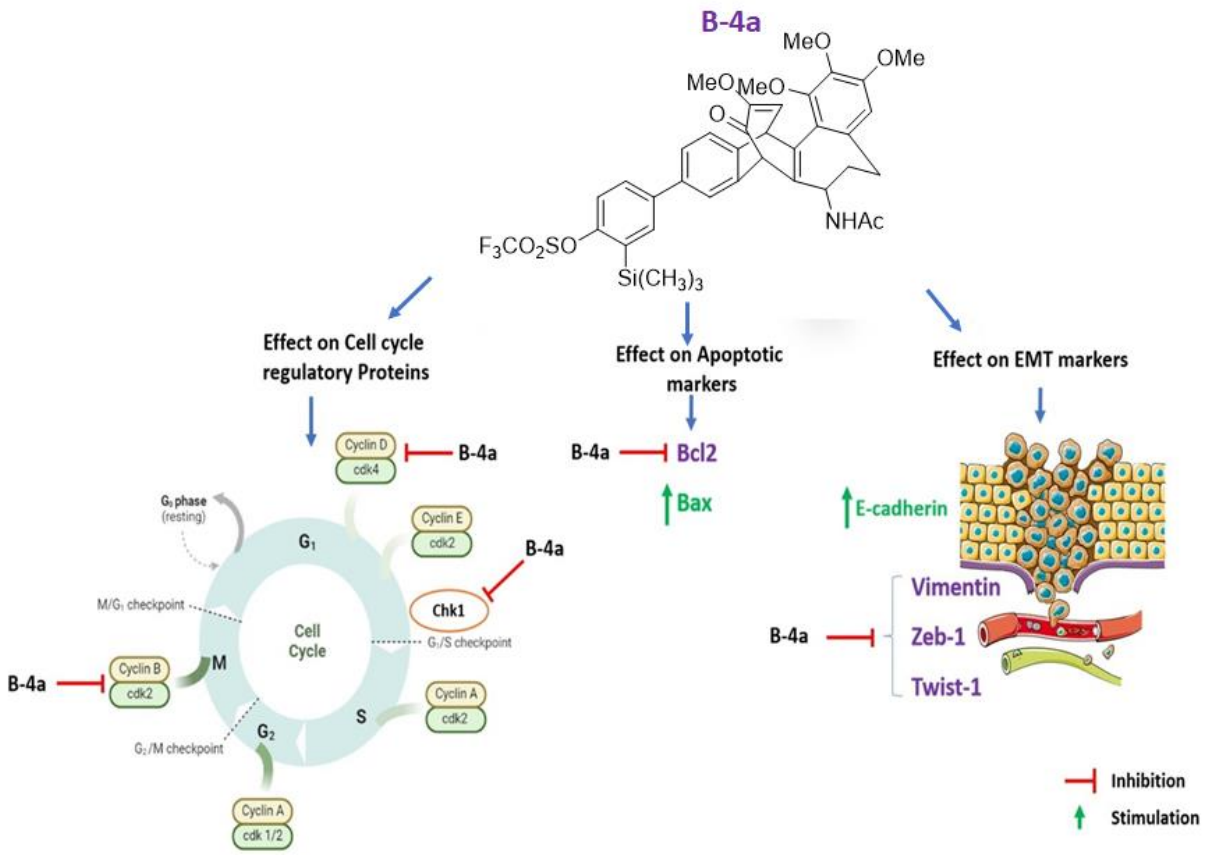

https://doi.org/10.26434/chemrxiv-2024-rs3lh **ORCID:** https://orcid.org/0000-0003-2378-3944 Content not peer-reviewed by ChemRxiv. **License:** CC BY-NC-ND 4.0

Abstract:

The anticancer potential of colchicine and its derivatives has garnered significant attention due to their ability to bind with tubulin, a critical cytoskeletal protein crucial for cell division's mitotic phase. In this study, we synthesized a new-generation library of colchicine derivatives via cycloaddition of colchicine utilizing position C-8 and C-12 diene system regioselectivity with aryne precursor to generate a small focussed library of derivatives. We assessed their anticancer activity against various cancer cell lines like MCF-7, MDA-MB-231, MDA-MB-453, and PC-3. Normal human embryonic kidney cell line HEK-293 was used to determine the toxicity. Among these derivatives, the silicon-tethered compound **B-4a** demonstrated the highest potency against breast cancer cells. Subsequent mechanistic studies revealed that **B-4a** effectively modulates cell cycle regulatory kinases (cdk-2 and cdk-4) and their associated cyclins (cyclin B1, cyclin D1), inducing apoptosis. Additionally, **B-4a** displayed a noteworthy impact on tubulin polymerization, distinct from the parent colchicine, and significantly disrupted the vimentin cytoskeleton, contributing to G1 arrest in breast cancer cells. Moreover, **B-4a** exhibited substantial anti-metastatic properties by inhibiting breast cancer cell migration and invasion. These effects were attributed to the down-regulation of major epithelial to mesenchymal transition (EMT) factors, including Vimentin and Twist-1, as well as the upregulation of the epithelial marker E-cadherin in an apoptosis-dependent manner.

Keywords: Tropolone alkaloid, cytoskeletal protein, anticancer, cell cycle arrest, epithelial to mesenchymal transition, programmed cell death.

Abbreviations: HRMS: high-resolution mass spectrometry; NMR: nuclear magnetic resonance; DFT: discrete Fourier transform; HPLC: high-performance liquid chromatography; MTT: 3-(4,5-dimethylthiazol-2yl)-2,5diphenyl tetrazolium bromide; DMSO: dimethyl sulphoxide; RIPA: radioimmunoprecipitation assay buffer; SDS-PAGE: sodium dodecyl sulfate-polyacrylamide gel electrophoresis; PVDF: polyvinylidene

https://doi.org/10.26434/chemrxiv-2024-rs3lh **ORCID:** https://orcid.org/0000-0003-2378-3944 Content not peer-reviewed by ChemRxiv. **License:** CC BY-NC-ND 4.0

difluoride; VEGF: vascular endothelial growth factor; EMT: epithelial to mesenchymal transition; FITC: fluorescein isothiocyanate; DAPI: 4',6-diamidino-2-phenylindole; BSA: bovine serum albumin; PBS: phosphate buffer saline; PBST: phosphate buffer saline tween-20; TBST: tris-buffer saline tween-20; FACS: fluorescence-activated cell sorting.

1. Introduction

Colchicine (**1**) is a bioactive natural product alkaloid, and an FDA-approved drug for the treatment of acute gout flares, familial Mediterranean fever, Behcet's disease, chondrocalcinosis, and other types of microcrystalline arthritis. It is a well-known antimitotic agent that binds to β-tubulin, destabilizes microtubules, and promotes depolymerization, leading to cell cycle arrest, apoptosis, and cell death. Today, this alkaloid can be obtained from both natural and synthetic sources. Naturally, it is isolated from the medicinal plant *Colchicum autumnale*, commonly known as autumn crocus, though it has been reported to be also found in other species like *Gloriosa superba* and *Gloriosa rothschildiana* [1]. Due to its relatively high toxicity to normal cells associated with adverse side effects, it has not been used in cancer chemotherapy. However, due to its mitotic properties, its skeleton has garnered a lot of interest from medicinal chemists and biologists alike to decipher the development of its derivatives which will have high potency and reduced toxicity [2].

In recent years, gynaecological cancers are the commonest cause of mortality in women worldwide [3]. Especially the incidences of breast cancer are immensely surging so the treatment of breast cancer becomes a great challenge for healthcare professionals urging for the rapid development of new generation therapeutics for the treatment of breast cancers preferably from natural sources. Cellular cytoskeletal-related proteins, for example, Tubulin play an important role in the regulation of mitotic catastrophe which is closely associated with the cellular proliferation and maintenance of cellular integrity [4]. Tubulin-

https://doi.org/10.26434/chemrxiv-2024-rs3lh **ORCID:** https://orcid.org/0000-0003-2378-3944 Content not peer-reviewed by ChemRxiv. **License:** CC BY-NC-ND 4.0

depolymerization is responsible for cell death and loss of cellular integrity. Structural optimization of a particular natural product sometimes becomes beneficial to enhance potency, favourable pharmacokinetic parameters, and most importantly reduce unwanted side effects. This approach though challenging, led to the emergence of numerous clinical candidates in the past by carrying out selective modifications on densely functionalized molecules [5]. However, this requires the development of efficient selective single-step transformation on a complex natural product thereby avoiding multistep transformations and protecting group manipulations.

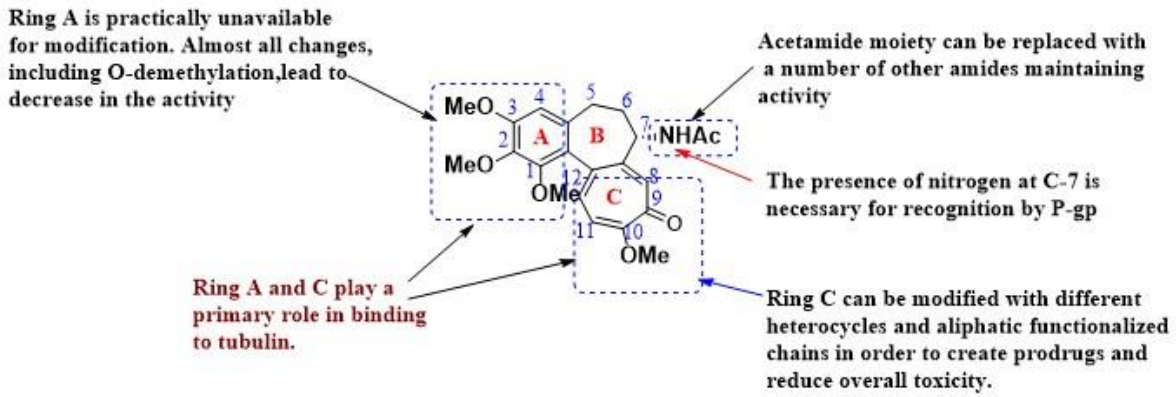

Figure 1: Structure and structural activity relationship of colchicine

Structurally, colchicine is a tricyclic system containing one 6-membered and two 7-membered rings with an (R)-stereogenic centre at the C-7 position (Figure 1). To overcome this issue, numerous structural variations have been performed to bring into more significant derivatization for the optimization of the various physiochemical properties at skeletal rings A, B, and C including side chain modifications [6]. The methoxy groups present on rings A and C are necessary for tubulin binding; therefore, any modification on these sites may not deliver promising results for enhancing the binding interaction with tubulin [7]. On the other hand, the N atom can be functionalized only if the presence and position of the N atom at C-7 remain intact which is necessary for the recognition of P-glycoprotein (Figure 1). Any

https://doi.org/10.26434/chemrxiv-2024-rs3lh ORCID: https://orcid.org/0000-0003-2378-3944 Content not peer-reviewed by ChemRxiv. License: CC BY-NC-ND 4.0

attempt to replace the N atom could lead to adducts not sticking to the P-gp binding [8]. Despite the previous modifications and wide scope for the structural diversity, a handful of work on its reaction with the aryne intermediates has been reported to date. Arynes are versatile reactive intermediates and precursors that offer the key advantage of rapid functionalization of natural products in a single operation. In addition, arynes are easy to generate *in situ*, and their use often results in the formation of C-C and C-X bonds in a regioselective manner involving various modes of reactions. The tropone moiety can act as a 4π component in Diels−Alder reaction, and react with electron-rich as well as electro-poor dienophiles to give access to bicyclo [3.2.2] compounds in a straightforward manner [9-11]. Arynes are highly electrophilic, hence act as strong dienophiles in the Diels-Alder reaction [11]. The synthetic utility of aryne and tropone moiety was first shown by Kende and co-workers in 1967 [12]. However, the scope of the reaction in this case was found to be limited with low yield to one example only and no attempt has been made to evaluate the anticancer properties of the synthesized adduct. Therefore, herein, we set to carry out the synthetic modification of colchicine in a simple and straightforward manner by attaching reactive aryne units via [4+2] cycloaddition which may enhance pi-pi interaction and hydrophobicity and thereafter evaluation of their anticancer activities against specific targets.

2.0 Chemistry synthesis

In colchicine, a substituted tropolone system exists which acts as a source of two dienes, so there is a possibility of the formation of two products. But, when arynes are used as dienophiles, it has been observed that only one diene (between C8 and C12) participated in the reaction, confirmed by NMR data of the possible products (Scheme 1). The cycloaddition reaction proceeds exclusively with the formation of the *endo* product leading to two regioisomeric forms. While the regioisomer formed in **B-1**, **B-3**, **B-5**, and **B-8** were observed

https://doi.org/10.26434/chemrxiv-2024-rs3lh **ORCID:** https://orcid.org/0000-0003-2378-3944 Content not peer-reviewed by ChemRxiv. **License:** CC BY-NC-ND 4.0

in trace amounts and could not be purified; sufficient amounts of regioisomers were formed in the case of **B-2a**, **B-4a**, **B-6a,** and **B-7a** forming **B-2b**, **B-4b**, **B-6b** and **B-7b.** The regioselectivity can be explained based on competing steric and electronic factors including aryne distortions. The arynes are affected when a substituent causes a geometrical distortion such that the geometry of the aryne resembles the transition state for nucleophilic attack on one of the carbons. Nonetheless, the exact reason behind this fact is still an important area of research.

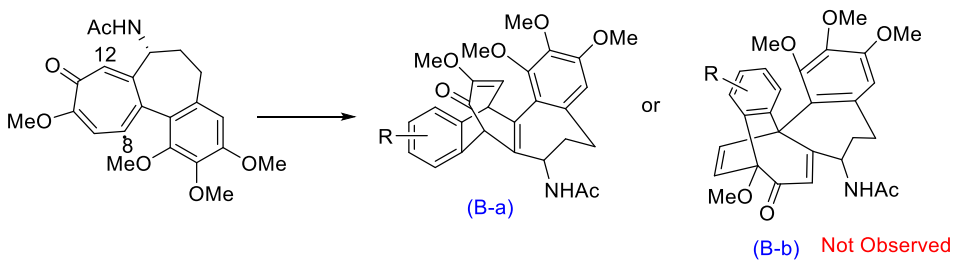

Scheme 1: Cycloaddition reaction of colchicine with benzyne precursor

Colchicine and substituted benzyne precursors were reacted in dry acetonitrile under inert conditions at room temperature. The reaction mixture was allowed to stir on a magnetic stirrer for four hours using cesium fluoride as a base which results in the formation of two products. The regioisomeric mixture was separated by using RP-HPLC (Reverse-Phase High-Performance Liquid Chromatography). The RP-HPLC was equipped with Agilent 1260 series having a PDA detector (UV detection at 215 and 254 nm), RP-prep C18 (Eclipse XBD-C18, 5µm, 9.4 × 250mm) column (column temp 30℃) with a flow rate of 2.5 ml/min and the gradient elution was performed with 60 to 80% MeOH in water as mobile phase for 25 minutes. Different substituted benzyne precursors were used in the cycloaddition reaction with colchicine **(Scheme 2)** and elucidated using ^{1}H and ^{13}C NMR and 2D NMR. Different substituents were chosen to facilitate the structural activity relationship analysis (SAR). All the products formed in the reaction were interpreted by ^{1}H and ^{13}C NMR, 2D NMR, and Mass. By comparing the ^{1}H-NMR data of (1), it has been shown that the signals of 8-H and

https://doi.org/10.26434/chemrxiv-2024-rs3lh **ORCID:** https://orcid.org/0000-0003-2378-3944 Content not peer-reviewed by ChemRxiv. **License:** CC BY-NC-ND 4.0

12-H of **B-4a** were shifted to higher fields, whereas the ^{13}C-NMR signals of C-8 and C-12 were found at δ 48.93.46 and δ 56.86 respectively, which confirms that the (4+2) cycloaddition had occurred Regio selectively at C-8 and C-12 position of colchicine.

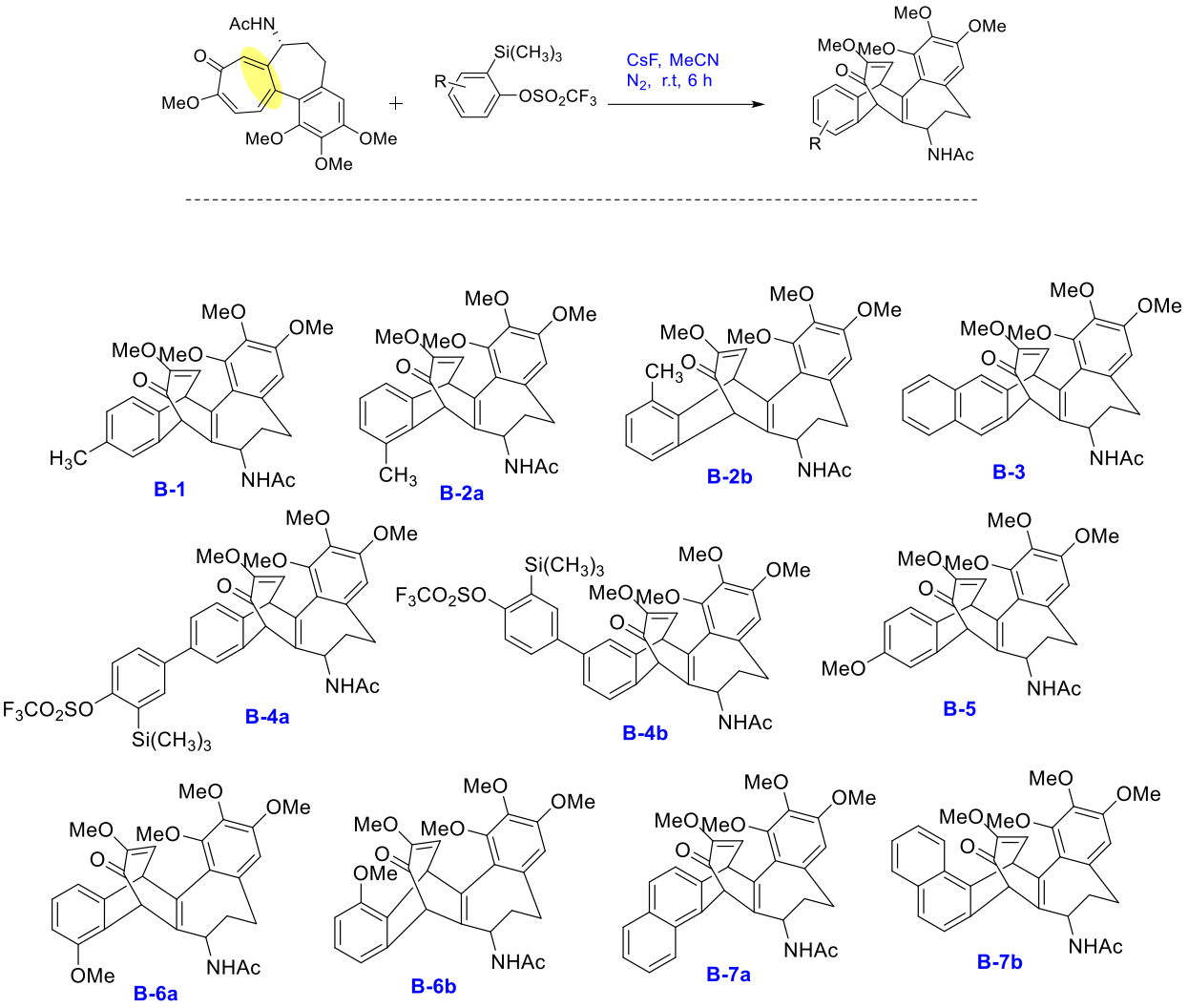

Scheme 2: Colchicine derivatives with different substituted benzyne precursors.

The structure and stereochemistry of colchicine analogues, herein for instance, compound **2a**, was confirmed by detailed analyses of HMBC spectra (See Supporting Information). Comparison of the ^{1}H and ^{13}C NMR spectrum of 2a and 2b with colchicine revealed the absence of 8, 12 diene signals in **2a**, the regioselectivity in **2a** and **2b** was supported by key correlations in HMBC spectrum (Scheme 3).

https://doi.org/10.26434/chemrxiv-2024-rs3lh **ORCID:** https://orcid.org/0000-0003-2378-3944 Content not peer-reviewed by ChemRxiv. **License:** CC BY-NC-ND 4.0

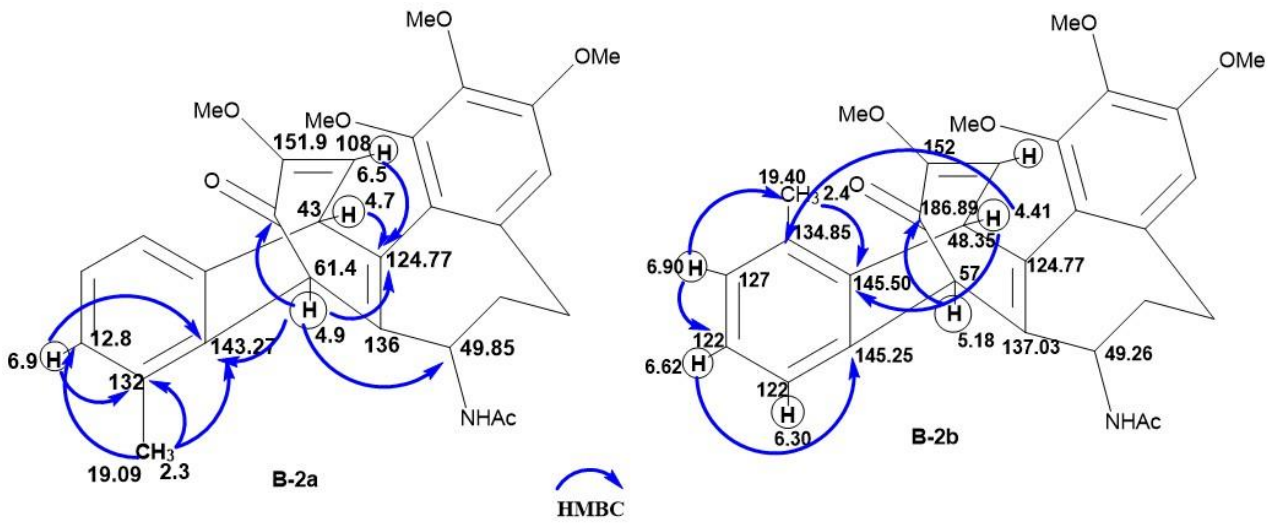

Scheme 3: HMBC Correlations of **B-2a** and **B-2b**

The HMBC correlations from H-8 (δH 4.93) to C-9 (δC 187.58), C-13 (δC 124.77), C-7 (δC 49.85) and C-14 (δC 143.27), from H-12 (δH 4.75) to C-13 (δC 124.77), from H-11 (δH 6.52) to C-13 (δC 124.77), from H-20 (δH 2.31) to C-15 (δC 132.07), C-16 (δC 128.17), C-14 (δC 143.27), and from H-16 (δH 6.92) to C-14 (δC 143.27), C-15 (δC 132.07) reveal the structure of 2a formed during the cycloaddition of substituted aryne with 8,12 diene of colchicines. Furthermore, signals in the **2b** were also assigned by HMBC correlations (Scheme 3) which unambiguously revealed the 2D structure of 2b. The HMBC correlations in 2b from H-8 (δ H 5.18) to C-9 (δC 187.58), from H-12 (δH 4.43) to C-18 (δC 134.85), C-19 (δC 145.50), from H-16 (δH 6.62) to C-14 (δC 145.25), from H-17 (δH 6.91) to C-16 (δC 122.05), and from H-20 (δ H 2.40) to C-19 (145.50) reveal the structure of **2b**. After the confirmation of all the structures and stereochemistry the given samples were submitted for their anti-cancer activity *in vitro*.

3. Biological investigations

3.1 Cell and cell culture

https://doi.org/10.26434/chemrxiv-2024-rs3lh **ORCID:** https://orcid.org/0000-0003-2378-3944 Content not peer-reviewed by ChemRxiv. **License:** CC BY-NC-ND 4.0

Human breast cancer cell lines (MCF-7, MDA-MB-231, MDA-MB-453), prostate cancer cell line (PC-3), and human embryonic kidney cell line (HEK-293) were procured from the European Collection of Cell Culture (ECACC). MCF-7, PC-3, and HEK-293 were cultured in RPMI 1640 media supplemented with 10% FBS, 100mg/ml streptomycin, and 100 IU penicillin and allowed to grow at 37°C in CO_2 incubator supplied with 5% CO_2. The breast cancer cell line MDA-MB-231 was allowed to grow in DMEM medium and MDA-MB-453 was allowed to grow in L-15 medium as per manufacturer's protocol.

3.2. Cell viability studies

Cells were seeded in 96 well plates at a concentration of 5×10^3 cells per well and allowed to grow for 24h. MTT assay was employed for the determination of the cell viability following the treatment of the cells with indicated concentrations of the derivatives of colchicine. Following incubation of the cells with compounds as indicated, MTT solution (2.5 mg/ml) was added and cells were further kept at 37°C for 4.0 hrs. Next, cells were incubated with DMSO at room temperature for 10.0 min to solubilize the formazan derivatives, and the absorbance of formazan derivatives was determined using a microplate reader at 570 nm. The percentage viability was determined according to the protocol described [13].

3.3 Immunocytochemistry

To perform the immunocytochemistry, cells (MDA-MB-231 and MCF-7) were seeded on coverslips in a 6-well plate at a density of 5×10^5 cells per well and 3×10^4 cells per well in 8 well chamber slide. The cells were allowed to grow for 24.0 hrs at 37°C in a CO_2 incubator. Following the dose-dependent treatment (for 24.0 hrs) with colchicine, Flavopiridol hydrochloride, and B-4a, cells were washed thrice with PBS. Next, the cells were fixed with 4 % paraformaldehyde (pH=7.4) for 15 min, permeabilized with 0.3 % Triton X-100 for 10 min, and then blocked with 1% BSA for 30 min. Consequently, the cells were incubated with

https://doi.org/10.26434/chemrxiv-2024-rs3lh **ORCID:** https://orcid.org/0000-0003-2378-3944 Content not peer-reviewed by ChemRxiv. **License:** CC BY-NC-ND 4.0

primary antibody overnight at 4°C, at a dilution of 1:400, followed by washing with PBST and further incubation with secondary antibody (1:1000). After subsequent washing and mounting, the images were captured at 20× magnification under Floid Cell Imaging Station (Invitrogen). The list of antibodies used in the experiment is described in the Supplementary data.

3.4 Immunoblotting

For the immunoblotting studies, mammalian breast cancer cell lines MCF-7 and MDA-MB-231 were grown in cell culture 60 mm petri dish at the density of 2×10^5 cells per dish and treated with the B-4a, colchicine, and Flavopiridol hydrochloride at different concentrations. The cells were lysed with RIPA lysis buffer containing phosphatase and protease inhibitors and the total proteins in the samples were quantified by Bradford assay. Approximately 20-25 μg of protein were loaded and separated by SDS-PAGE gel electrophoresis. Protein was transferred on a PVDF membrane and blocked with 3% BSA for 1 hour and further incubated overnight with the primary antibody at 4°C. The dilutions for primary antibodies were cdk-2 (1:1000), cdk-4 (1:1000), cyclin D1 (1:1000), cyclin B1 (1:1000), chk-1 (1:1000), zeb-1 (1:1000), e-cadherin (1:2000), twist (1:1000) and beta-actin (1:3000). The blots were washed with TBST and further incubated with secondary antibodies anti-mouse IgG (1:3000), and anti-rabbit IgG (1:3000) for 2h at room temperature. Finally, the blots were developed by using an ECL clarity substrate (Bio-Rad cat no. 1705061) in the Chemidoc system (Syngene Chemidoc XRQ, GeneSys software). The densitometric analysis of different blots was done by using Image J analysis software (National Institute of Health, Bethesda, Maryland, USA).

3.5 Fluorescence-activated cell sorting analysis

https://doi.org/10.26434/chemrxiv-2024-rs3lh **ORCID:** https://orcid.org/0000-0003-2378-3944 Content not peer-reviewed by ChemRxiv. **License:** CC BY-NC-ND 4.0

Cell cycle analysis was performed as per the standardized protocol [14]. Breast cancer cells (MCF-7/5×10^6 cells per well) seeded in a 6-well culture plate were exposed to colchicine, Flavopiridol hydrochloride, and B-4a as indicated. Post-treatment, cells were harvested and incubated with a staining solution (Propidium iodide (1mg/ml)) for 15 min according to the manufacturer's protocol. Further, cells were analyzed by flow cytometer (BD Cell Quest Pro software).

3.6 Wound healing (Scratch motility) assay

A wound healing (scratch motility) assay was performed according to the protocol established by our group [15]. MCF-7 cells were seeded in a 6-well plate at the density of 1×10^6 cells per well and allowed to grow for 24.0 hrs. After 24.0 hrs, the confluent monolayer was scratched with a sterile micropipette tip (20−200 µl), and the detached cells were removed by gentle washing with a serum-free medium. Subsequently, cells were treated with different concentrations of compound B-4a, colchicine, Flavopiridol hydrochloride, and vehicle, in starvation medium for another 48 h. Wounded areas were photographed by using an inverted microscope at 10× magnification and the total % area under the wound was analyzed by using the wound healing tool of Fiji distribution of Image J software.

3.7 Transient transfection

MCF-7 cells were seeded (0.5×10^5) in 60 mm culture dishes and next morning transfected with vector/ (purchased from Addgene, Massachusetts, USA) using lipofectamine 3000 (Life Technologies, Carlsberg, CA, USA) as per the manufacturer's guidelines. Forty-eight hours post-transfection, cells were treated with Flavopiridol hydrochloride, and **B-4a** for the indicated time. After incubation, harvested cells were subjected to western blotting.

3.8 Fluorescent Gelatin degradation assay

https://doi.org/10.26434/chemrxiv-2024-rs3lh **ORCID:** https://orcid.org/0000-0003-2378-3944 Content not peer-reviewed by ChemRxiv. **License:** CC BY-NC-ND 4.0

FITC-Gelatin was performed according to the previously standardized protocol. To check the degradation of the FITC gelatin matrix and invadopodia formation, the MDA-MB-231 cells were cultured on FITC gelatin-coated coverslips at the density of 1×10^5 cells/coverslip and allowed to grow for 12.0 hrs. After 12.0 hrs, cells were treated with B-4a, Flavopiridol hydrochloride, and colchicine for 24.0 hrs. Following treatment, the cells were observed under Floid Cell Imaging Station to determine the gelatin degradation and invadopodia formation, and the images were processed for estimating the threshold area of degradation by the Image J software.

3.9 Statistical analysis

The data were represented as Mean ± S.D. of at least three independent experiments, $IC_{50,}$ and *p-value* were calculated by using GraphPad Prism (GraphPad Prism software, USA). One-way ANOVA and *student t*-test were employed to compare the data sets. $P\ values \leq$ 0.001 were used as significant and ns for nonsignificant.

4.0 Results

4.1 Design, synthesis, and evaluation of cytotoxicity of Colchicine derivatives

Colchicine is known for its micro-tubulin polymerization inhibiting activity and is the drug of choice for the treatment of gout [4,16]. It has a narrow therapeutic index and is highly toxic to normal cells. Many of its derivatives have been reported as anticancer agents (6, 17-19). To increase its tumor specificity and to reduce toxicity, new generation colchicine derivatives were synthesized. The chemical structures of various derivatives are shown in **Scheme 2**. All structures were characterized by HRMS and NMR; the data is included in the Supplementary section**.** To evaluate the cytotoxicity of colchicine derivatives, an MTT assay was performed against different mammalian cancerous and non-cancerous cell lines. The IC_{50} value of the derivatives was represented in **Table 1**. Normal human embryonic kidney cell line Hek-293

https://doi.org/10.26434/chemrxiv-2024-rs3lh **ORCID:** https://orcid.org/0000-0003-2378-3944 Content not peer-reviewed by ChemRxiv. **License:** CC BY-NC-ND 4.0

was used to check the toxicity. The cytotoxicity of different derivatives of colchicine against the different cancerous cell lines was compared with the parent molecule as well as with each other. It is noteworthy that adducts having more than one aromatic ring such as biphenyl or naphthalyl adducts (**B-3, B-4a, B-4b, B-7b**) exhibited higher potency in the MCF-7 cell line. Further, the presence of silicon in the biphenyl moiety significantly enhances the anticancer activity (**B-4a, B-4b**). Compound **B-4a** was found to be the most potent analogue of colchicine across all the cancer cell lines tested. It is worth mentioning that, compound **B-4a** was found to be substantially less toxic (IC_{50} value of 30.7±2.24) to normal cells (Hek-293) *in vitro* as compared to the parent molecule (IC_{50} value of 5.4±0.851) making it more acceptable for lead generation. Further, diligent analysis of the screening data, it was evident that compound **B-4a** showed broad spectrum anticancer activities against various cancer cell lines (MCF-7, MDA-MB-231, MDA-MB-453, and PC-3). Accordingly, compound **B-4a** was taken up further for mechanistic studies.

Table 1. IC_{50} values for the different derivatives of Colchicine screened against various cell lines.

https://doi.org/10.26434/chemrxiv-2024-rs3lh **ORCID:** https://orcid.org/0000-0003-2378-3944 Content not peer-reviewed by ChemRxiv. **License:** CC BY-NC-ND 4.0

S. No.	Compound code	MDA-MB-231 IC_{50} (µM) ± SD)	MDA-MB-453 IC_{50} (µM) ± SD)	MCF-7 IC_{50} (µM) ± SD)	PC-3 IC_{50} (µM) ± SD)	HEK293 IC_{50} (µM) ± SD)
1	B-1	>100	>100	>100	10.61 ± 0.288	18.92 ± 0.608
2	B-2a	22.65 ± 0.321	16.6 ± 0.292	>100	14.4 ± 0.150	23.5 ± 0.503
3	B-2b	37.5 ± 0.191	33.8 ± 0.152	>100	13.3 ± 0.180	21.2 ± 0.113
4	B-3	15.78 ± 0.378	16.0 ± 0.015	52.9 ± 0.409	6.74 ± 0.062	8.75 ± 0.731
5	**B-4a**	**4.97 ± 0.406**	**5.27 ± 0.115**	**4.69 ± 0.035**	**5.87 ± 0.024**	**30.7 ± 2.24**
6	B-4b	5.9 ± 0.152	5.35 ± 0.057	11.44 ± 0.021	7.62 ± 0.056	22.1 ± 1.512
7	B-5	>100	>100	>100	12.79 ± 0.051	19.6 ± 0.763
8	B-6a	26.34 ± 0.361	18.7 ± 0.305	>100	14.73 ± 0.058	18.6 ± 0.550
9	B-6b	23.4 ± 0.211	23.9 ± 0.209	87.3 ± 0.083	16.8 ± 0.078	23.9 ± 0.270
10	B-7a	34.03 ± 0.324	40.5 ± 0.118	88.4 ± 0.153	22.71 ± 0.230	9.16 ± 0.305
11	B-7b	14.5 ± 0.324	37.2 ± 0.118	18.2 ± 0.523	17.6 ± 0.170	12.8 ± 0.425
12	Colchicine	7.69 ± 0.264	5.75 ± 0.115	0.47 ± 0.028	0.04 ± 0.059	5.4 ± 0.851

4.2 B-4a negatively modulated the expression of the cell-cycle regulatory proteins

Normal cell cycle regulators, like cyclins, and cyclin-dependent kinases (cdks) have been investigated as potential targets for the treatment of cancer [20]. The cyclin-dependent

https://doi.org/10.26434/chemrxiv-2024-rs3lh ORCID: https://orcid.org/0000-0003-2378-3944 Content not peer-reviewed by ChemRxiv. License: CC BY-NC-ND 4.0

kinases form a complex with respective regulatory cyclin proteins and these complexes are responsible for the progression of the cell cycle [21]. Most conventional chemotherapeutics induce apoptosis by targeting positive regulators of the cell cycle. Another important mechanism behind the G_1 checkpoint induction is the rapid degradation of cyclin D1 after exposure to any chemotherapeutics and radiations [22]. Inhibition of cdk2/cyclin B1 complex and cdk4/cyclin D1 complex is responsible for cell cycle arrest as well as cell growth inhibition. Although Colchicine exhibits strong antimitotic properties, the immunoblotting study was performed to investigate the effect of the active compound **B-4a** (**Figure 2A & B)** on the cell cycle regulatory proteins. The expression of cell cycle regulatory proteins such as cyclin-dependent kinases (cdk-2, cdk-4), cyclin D1, cyclin B1, and chk1 was examined in the mammalian breast cancer cell lines (MCF-7 and MDA-MB-231) following treatment with compound **B-4a** and compared with the standard cyclin-dependent kinase inhibitor (Flavopiridol hydrochloride) and with the parent compound (colchicine). Our findings revealed a significant downregulation of the expression of cdk-2, cdk-4, cyclin D1, cyclin B1, and chk1 in the presence of compound **B-4a** in MCF-7 and MDA-MB-231 cells in a dose-dependent manner (**Figure 2C & D).** Further, compound **B-4a** significantly attenuated the expression of anti-apoptotic marker Bcl-2 and augmented pro-apoptotic marker Bax in a dose-dependent manner in MCF-7 (Figure 2C) as well as MDA-MB-231 cell line (**Figure 2D**). As expected, treatment with positive control flavopiridol hydrochloride also attenuated the cdk-2 and cdk-4 levels whereas parent molecule colchicine had negligible effects on cdk-2 and cdk-4 expression (**Figure S1)**.

https://doi.org/10.26434/chemrxiv-2024-rs3lh **ORCID:** https://orcid.org/0000-0003-2378-3944 Content not peer-reviewed by ChemRxiv. **License:** CC BY-NC-ND 4.0

Figure 2.

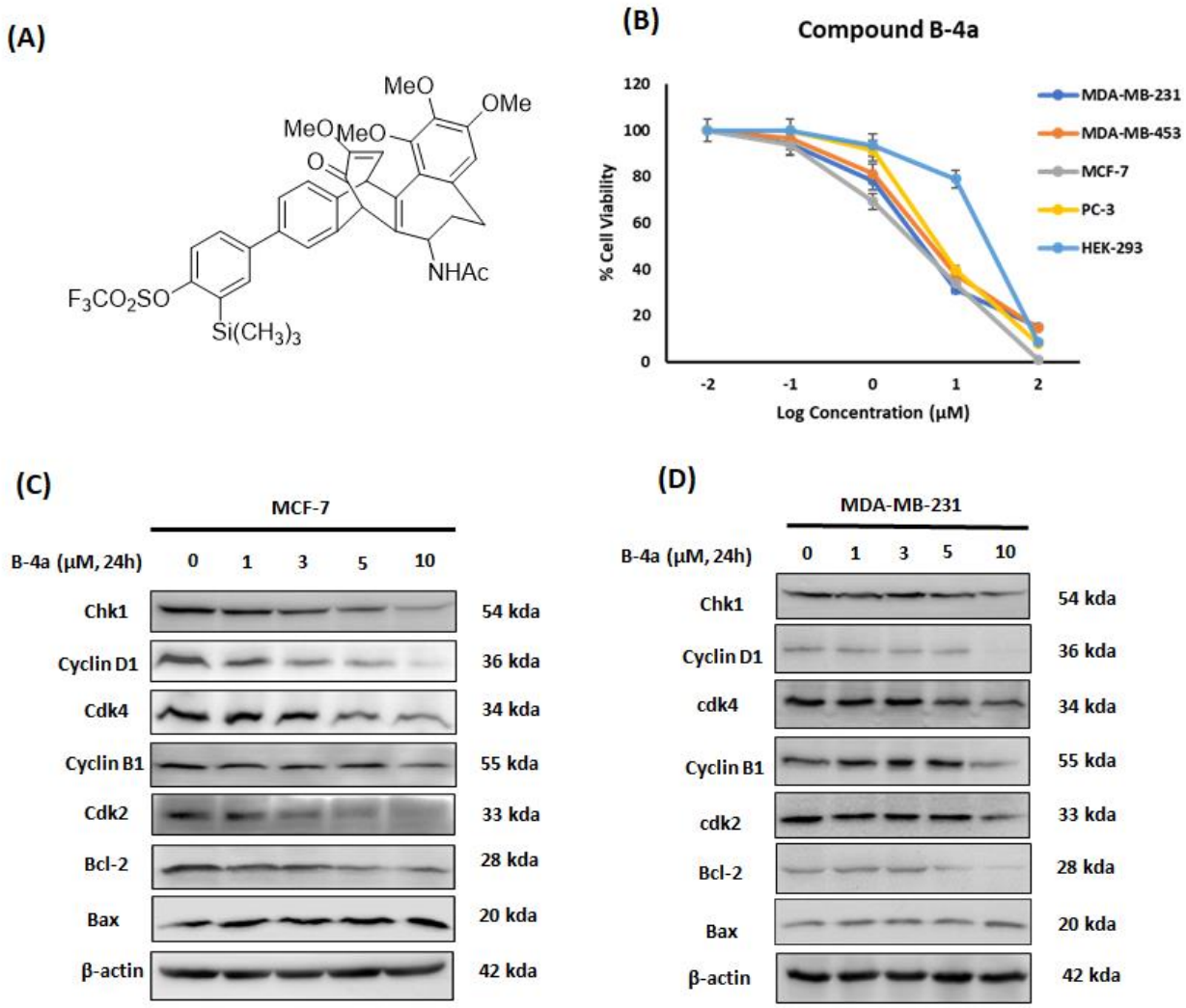

4.3 B-4a abrogated tubulin polymerization along with diminishing vimentin cytoskeleton

Microtubules are filamentous cytoskeletal proteins, conferring vital roles in spindle formation, cell division, proliferation, trafficking, signaling, and migration of cancer cells [23]. Natural products that modulate microtubule structures such as vinca alkaloids (vinblastine, vincristine) and taxanes (paclitaxel, docetaxel) are important chemotherapeutic agents for the treatment of cancer [24]. Colchicine at a low concentration can cause tubulin

https://doi.org/10.26434/chemrxiv-2024-rs3lh ORCID: https://orcid.org/0000-0003-2378-3944 Content not peer-reviewed by ChemRxiv. License: CC BY-NC-ND 4.0

depolymerization and further lead to cell death [16]. Therefore, we were curious to examine the effects of **B-4a** on tubulin polymerization. Interestingly, through our immunocytochemistry results, we observed normal organization of the microtubule network around the nucleus in vehicle-treated cells, and in contrast, a sharp decrease in microtubule polymerization was observed in cells treated with **B-4a** compared to positive control flavopiridol hydrochloride in a dose-dependent manner (**Figure 3A & C**). Moreover, the cytoskeleton protein vimentin plays a crucial role in cancer cell survival and proliferation. Vimentin is the most important and widely expressed type III intermediate filament in cells of mesenchymal origin. It plays a vital role in cellular signaling and the downstream signaling mediated for rapid cancer cell transformation. Therefore, we opted for checking the effects of **B-4a** on the vimentin cytoskeleton and our results consistently unleashed that vimentin intermediate filaments surrounded the nucleus and radiated out from the nucleus to the cell periphery, terminating near points of contact between adjacent cells in vehicle-treated cells. Strikingly, compared to control (colchicine), **B-4a** treatment caused vimentin intermediate filaments to collapse and the vimentin cytoskeleton network was restricted between nuclear and cell membranes (**Figure 3B & D).**

Figure 3.

https://doi.org/10.26434/chemrxiv-2024-rs3lh **ORCID:** https://orcid.org/0000-0003-2378-3944 Content not peer-reviewed by ChemRxiv. **License:** CC BY-NC-ND 4.0

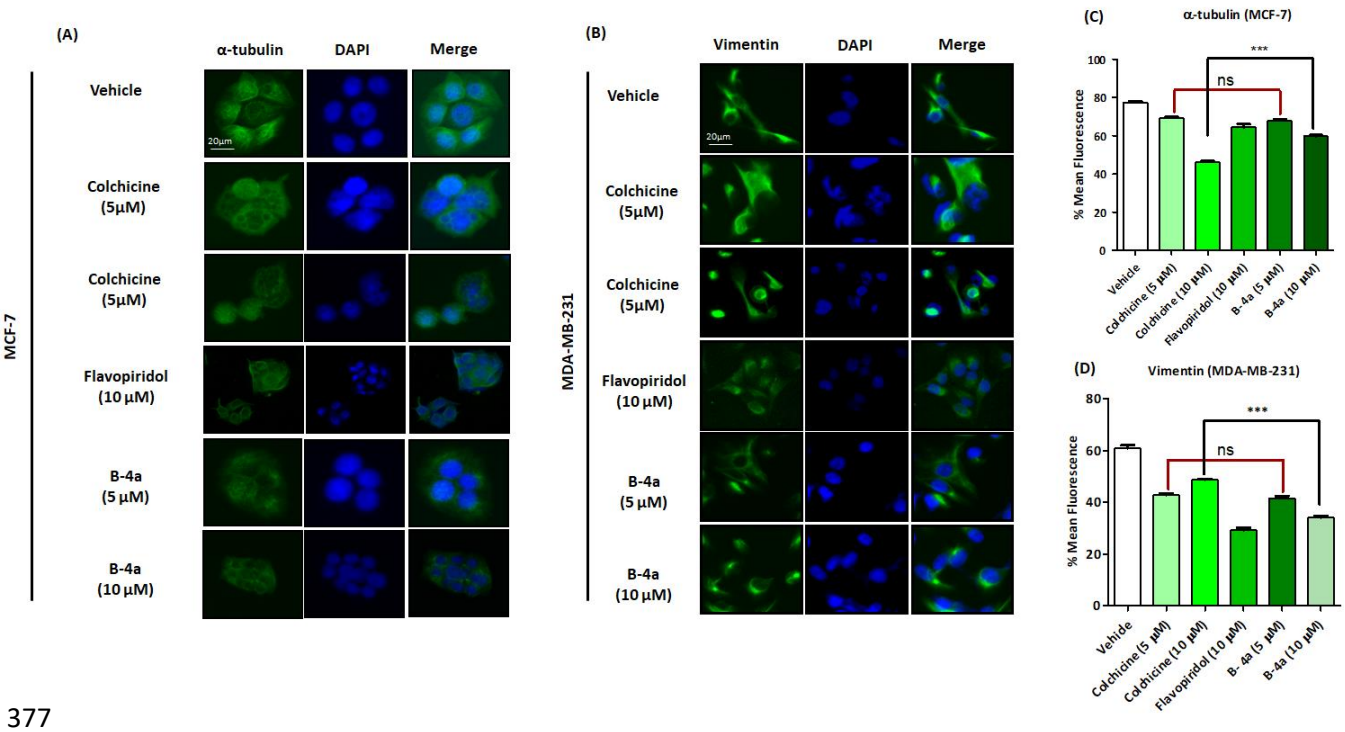

4.4 Compound B-4a triggered cell cycle arrest and apoptosis

The previous results elucidated that **B-4a** treatment led to the downregulation of cell cycle regulatory proteins. Accordingly, we sought to investigate whether compound **B-4a** could provoke cell cycle arrest and consequent apoptosis. We performed Annexin V-PI analysis for the assessment of cell cycle demonstrating that the treatment with **B-4a** induced cell cycle arrest of MCF-7 cells (**Figure 4A**). Since the flow cytometric method of assessing apoptosis renders an accurate determination of apoptotic index as well as cellular DNA content in cell cycle phases, we carried out cell cycle analysis in MCF-7 cells. Our flow cytometric data demonstrated a steady-state G1 arrest in cells treated with 5 µM of **B-4a (62.86%)** and 10 µM of **B-4a (65.78%)** compared to control. Positive control Flavopiridol hydrochloride triggered S phase arrest and colchicine triggered G2/M arrest in the same experiment. To validate our cell cycle results, we performed DAPI analysis to characterize the nuclear morphology in the presence of compound **B-4a** and the results showed distinguished

https://doi.org/10.26434/chemrxiv-2024-rs3lh **ORCID:** https://orcid.org/0000-0003-2378-3944 Content not peer-reviewed by ChemRxiv. **License:** CC BY-NC-ND 4.0

condensed nuclei following **B-4a** treatment. Additionally, flavopiridol hydrochloride also induced apoptotic condensed nuclei phenotype (**Figure 4B).**

Figure 4.

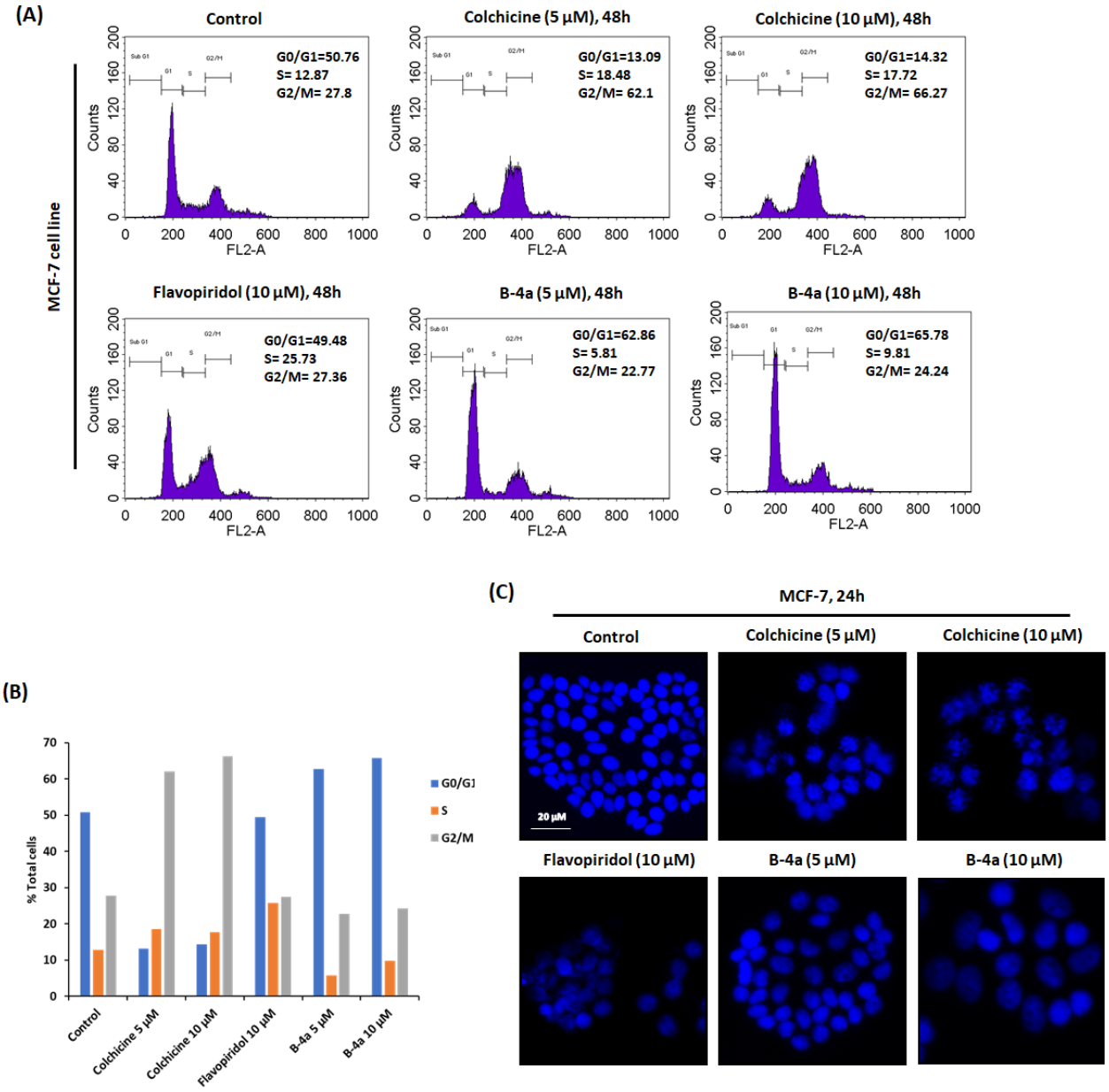

4.5 B-4a treatment abolishes epithelial to mesenchymal transition and migration of breast cancer cells

https://doi.org/10.26434/chemrxiv-2024-rs3lh **ORCID:** https://orcid.org/0000-0003-2378-3944 Content not peer-reviewed by ChemRxiv. **License:** CC BY-NC-ND 4.0

Epithelial to mesenchymal transition is the commonest cause of tumorigenesis and is responsible for drug resistance [25, 26]. Downregulation of epithelial marker E-cadherin and upregulation of mesenchymal markers such as vimentin, N-cadherin, and the upregulation of certain transcription factors like Zeb-1, Twist-1 are the essential leading events in the progression of EMT [27, 29]. An immunoblotting study was performed to investigate the effect of compound **B-4a** on the EMT markers. The expression of E-cadherin, Zeb-1, Vimentin, and Twist-1 was examined in the breast cancer cells (MCF-7 and MDA-MB-231 cells) following treatment with **B-4a**. Our findings revealed a significant upregulation of E-cadherin in the MCF-7 and MDA-MB-231 cells exposed to compound **B-4a** (**Figure 5 A & B**) while a significant downregulation of the transcription factors (Zeb-1, Twist-1) was observed in the same cells in presence of **B-4a** (**Figure 5 A & B**). Subsequently, the downregulation of Vimentin was also observed in the MDA-MB-231 cells treated with **B-4a**. Additionally, we have checked the effect of **B-4a** on the migration of cancer cells by wound healing (scratch motility) assay. A wound-healing assay was carried out to demonstrate whether compound **B-4a** could halt the motility of MCF-7 cells. Following 48 h of incubation with 5 and 10 μM **B-4a**, the motility of MCF-7 cells attenuated significantly ($p < 0.05$), similar to positive control flavopiridol hydrochloride (Figure 2A), whereas the cells incubated with vehicle extensively migrated through the scratched area to close the wound (**Figure 5 D & E**). Our findings implied that **B-4a** abolished the migration of MCF-7 cells (**Figure 5 D & E**). Additionally, we have performed a FITC gelatin degradation assay to determine the effect of **B-4a** on the formation of invadopodia/filopodia and gelatin degradation. The results of the FITC gelatin degradation assay implied that **B-4a** treatment conferred a considerable decrease in the gelatine degradation of the basement matrix as compared to the vehicle-treated cells. The reduction in total degradation area following **B-4a** treatment was significantly lower compared to colchicine and Flavopiridol hydrochloride since we did not

https://doi.org/10.26434/chemrxiv-2024-rs3lh **ORCID:** https://orcid.org/0000-0003-2378-3944 Content not peer-reviewed by ChemRxiv. **License:** CC BY-NC-ND 4.0

identify any significant change in the matrix degradation in the cells treated with Flavopiridol hydrochloride. Hence, **B-4a** treatment in MDA-MB-231 cells significantly diminished the matrix gelatine degradation area as compared to the Flavopiridol hydrochloride (**Figure 5 C**).

Figure 5.

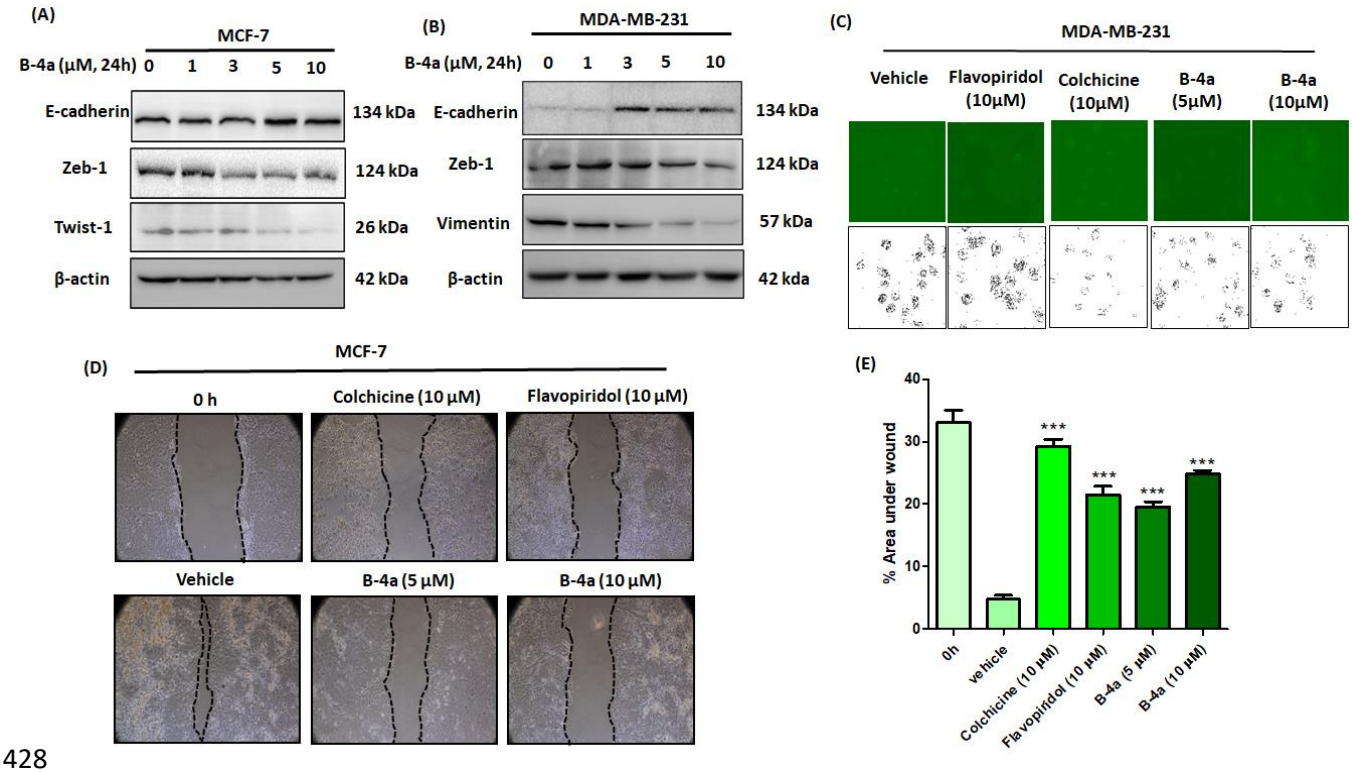

4.6 B-4a triggers anti-EMT (Epithelial to Mesenchymal Transition) responses via induction of apoptosis

Next, we sought to examine whether the inhibition of epithelial to mesenchymal transition of breast cancer cells by compound **B-4a** was due to the induction of apoptosis and how the cell cycle regulatory cdk-2, cdk-4, cyclin B1, and cyclin D1 were involved in that process. To do that, MCF-7 and MDA-MB-231 cells were first pre-treated with VEGF (cell motility inducer) for 2 hours followed by **B-4a** treatment (24.0 hrs) and second co-treatment with VEGF plus **B-4a** for 24h. Flavopiridol hydrochloride was used as a positive control to compare the kinase inhibitory activity of compound **B-4a**. The findings of immunoblotting data

https://doi.org/10.26434/chemrxiv-2024-rs3lh ORCID: https://orcid.org/0000-0003-2378-3944 Content not peer-reviewed by ChemRxiv. License: CC BY-NC-ND 4.0

demonstrated that compound **B-4a** significantly abolished the expression of cdk-2, cdk-4, cyclin B1, and cyclin D1 in the MCF-7 and MDA-MB-231 cells only when co-treated with VEGF **(Figure 6 A & B)**. Additionally, co-treatment of VEGF and **B-4a** diminished the anti-apoptotic Bcl-2 level in both cell lines. Further, we sought to examine the effects of **B-4a** on ectopic cdk-2 and cdk-4 proteins since these cdk-2 and cdk-4 expressions are adequately high in diverse cancers. To do this, we transfected MCF-7 cells with pCMV-cdk2 and pCMV-cdk4 plasmids and treated them with compound **B-4a.** The immunoblot results revealed a significant attenuation of ectopic cdk2 and cdk4 and corresponding cyclin B1, and cyclin D1expression in the presence of **B-4a** suggesting profound modulation of cell cycle regulatory markers by **B-4a.** Additionally, **B-4a** treatment abolished the epithelial to mesenchymal transition factor Twist 1 along with a sharp increase in pro-apoptotic Bax level implying that B-4a mediated down-modulation of EMT cascade was apoptosis dependent **(Figure 6 C & D)**.

https://doi.org/10.26434/chemrxiv-2024-rs3lh **ORCID:** https://orcid.org/0000-0003-2378-3944 Content not peer-reviewed by ChemRxiv. **License:** CC BY-NC-ND 4.0

460 **Figure 6.**

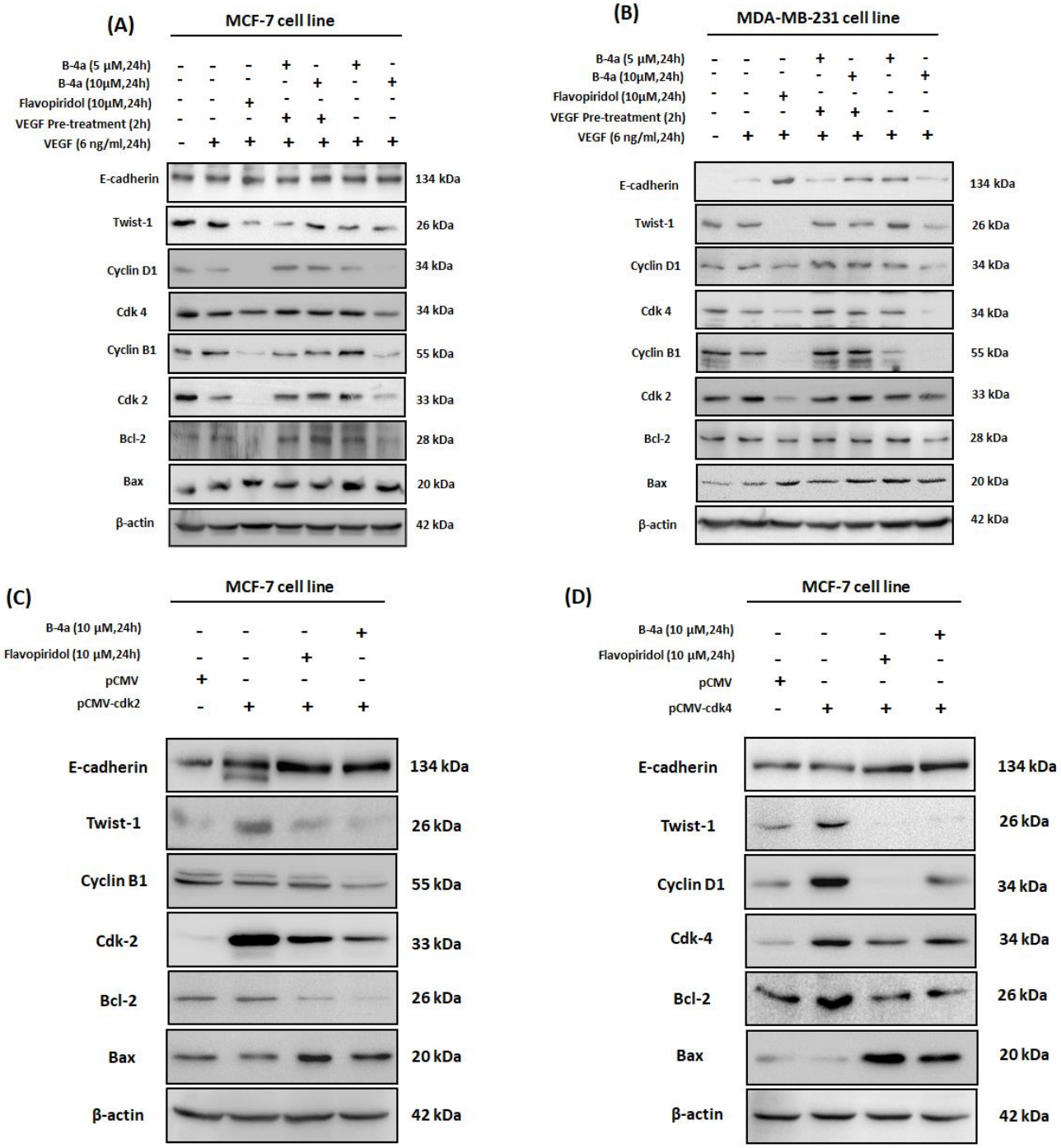

461

462

463

464

https://doi.org/10.26434/chemrxiv-2024-rs3lh **ORCID:** https://orcid.org/0000-0003-2378-3944 Content not peer-reviewed by ChemRxiv. **License:** CC BY-NC-ND 4.0

Figure 7.

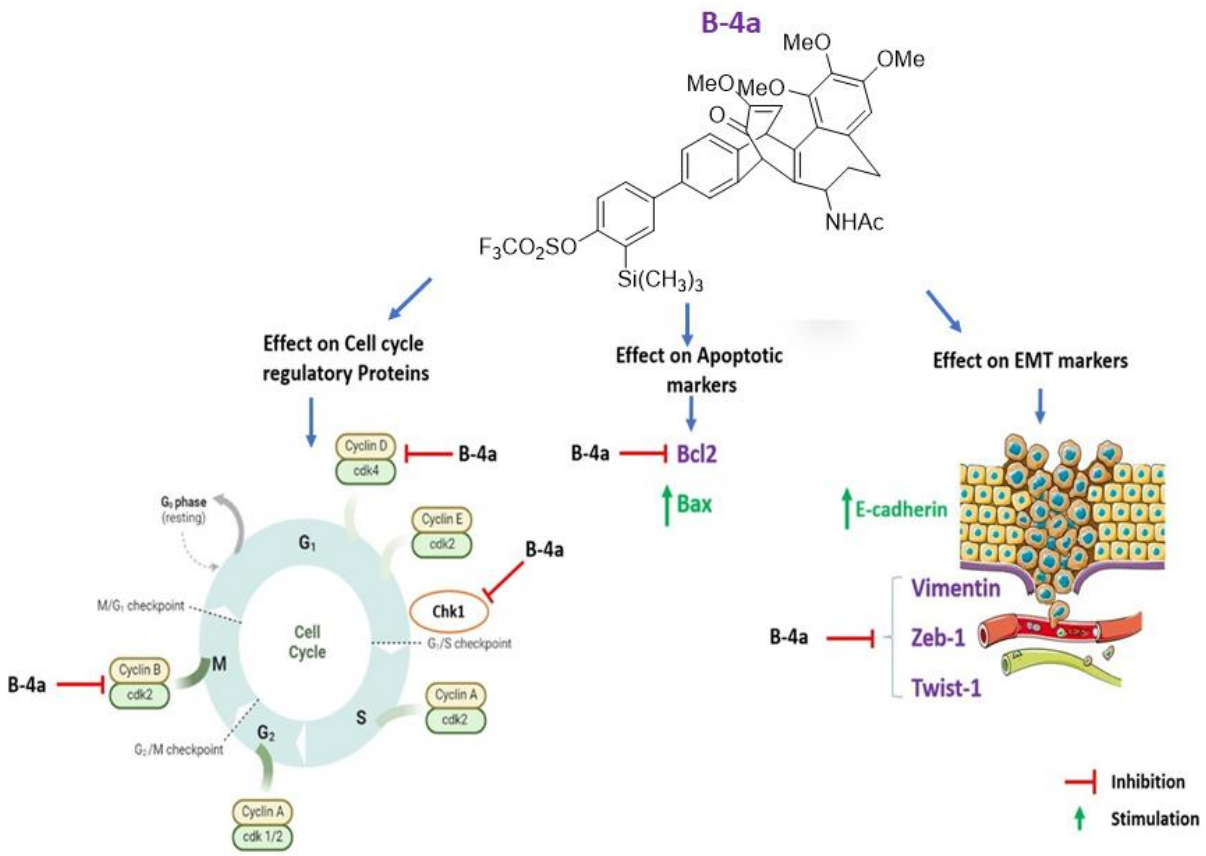

5.0 Discussion

Colchicine continues to grab attention as a drug and was approved by FDA (Food and Drug Administration) for the treatment of gout in 2009 [6]. Its derivatives are also well known for the treatment of certain inflammatory [30], dermatological [31] and cardiovascular disorders [32]. The interaction of colchicine and its derivatives necessitates at least one hydrogen acceptor, a planar group, and two hydrophobic centers for effective binding with tubulin [33, 34] whereas with unpolymerized tubulin heterodimers and destabilizes the microtubule polymerization resulting in reduced cell mortality in certain types of cells by mitotic arrest [35].

https://doi.org/10.26434/chemrxiv-2024-rs3lh **ORCID:** https://orcid.org/0000-0003-2378-3944 Content not peer-reviewed by ChemRxiv. **License:** CC BY-NC-ND 4.0

In our present work, various derivatives of colchicine were synthesized and screened for their anticancer potential against various mammalian cancerous cell lines. We decided to perform [4+2] cycloaddition reaction utilizing the tropolone moiety at ring C as a diene in the presence of arynes as dienophiles. There are two conjugated diene systems namely C-8/C-12 and C-10/C-12. Gratifyingly, we got one only adduct regioselectively involving C-8/C-12 double bond with unsubstituted benzyne. As anticipated, in the case of substituted arynes we observed a mixture of regioisomers based on the substitution at aryne moiety which required HPLC purification for separation and characterization. Finally, we have successfully generated a small focussed library of eleven adducts. According to the cytotoxicity study performed, the compound **B-4a** was found to be a potent anticancer derivative of colchicine having the best IC_{50} values against MDA-MB-231 and MCF-7 cells and which was further investigated for the mechanistic studies. We found that compound-**B4a** is a potent inhibitor of cyclin-dependent kinases and it significantly abrogated the expression of cdk2 and cdk4 in both MCF-7 and MDA-MB-231 cells. In addition, immunoblotting, and immunocytochemistry studies of compound **B-4a** revealed its effect on the proteins responsible for epithelial-to-mesenchymal transition and apoptosis. According to our findings, the compound **B-4a** significantly inhibited the EMT markers Vimentin, Zeb-1, and Twist-1. **B-4a** also diminished Bcl-2 proteins and was responsible for the programmed cell death in both MCF-7 and MDA-MB-231 cells. However, the compound **B-4a** did not results in tubulin depolymerization as compared to the parent molecule in MCF-7 cells. In comparison to colchicine, the active derivative (compound **B-4a**) has a potent effect on the cell cycle regulatory proteins. Through our investigations, we have elucidated the mechanism of action of compound **B-4a** as shown in the schematic diagram **(Figure 7).** As per the findings, detailed investigations will be required to elucidate the mechanism of action of compound **B-4a**.

https://doi.org/10.26434/chemrxiv-2024-rs3lh **ORCID:** https://orcid.org/0000-0003-2378-3944 Content not peer-reviewed by ChemRxiv. **License:** CC BY-NC-ND 4.0

Conclusion

In this study, the silicon-tethered colchicine derivative **B-4a** exhibits a potent anti-cancer effects against breast cancer cell lines whereby demonstrating a high efficacy in modulating key cell cycle regulatory kinases, including apotosis, and disruting tubulin polymerization out of all derivatives synthesized. Its also noteworthy that anti-metastatic properties were observed, attributed to down-regulating of epithelial to mechenchymal transition (EMT) factors via induction of apoptosis. **B-4a** which was found to be substantially less toxic to normal cells (Hek-293) as compared to the parent colchicine molecule, this would attribute to silicon-tithered derivative making it more acceptable for lead generation. The advantages of incorporation of silicon into the molecules can impact on important parameters like potency, selectivity, pharmacokinectic and pharmacodynamic properties are well evident. This findings warrants **B-4a** as a promising lead for further investigation in medicinal chemistry properties and breast cancer therepy.

Author contribution

WIL: Design and synthesis, methodology, manuscript writing & editing; JC: investigations, methodology, formal analysis, data analysis, manuscript writing & editing; PK: data analysis, manuscript writing & editing; ZA: manuscript review; DM: conceptualization, supervision, review, and editing of the manuscript, AG: supervision, manuscript writing, review, and editing: JSMHA: conceptualization, supervision, manuscript review, and editing.

Acknowledgments

The work was supported by the internal institutional grant (HCP-007, HCP-40, and MLP-110017) from the Council of Scientific and Industrial Research (CSIR), Govt. of India. We thank our Director, Dr. Zabeer Ahmed for encouraging us to accomplish this work. WIL and JC thank the Council of Scientific and Industrial Research for providing the fellowship. The institutional publication number of the study is CSIR-IIIM/IPR/00573.

https://doi.org/10.26434/chemrxiv-2024-rs3lh **ORCID:** https://orcid.org/0000-0003-2378-3944 Content not peer-reviewed by ChemRxiv. **License:** CC BY-NC-ND 4.0

Conflict of Interest

The authors declare no conflicts of interest.

References

1. a). Canela, M. D.; Pérez-Pérez, M. J.; Noppen, S.; Sáez-Calvo, G.; Díaz, J. F.; Camarasa, M. J.; Liekens, S.; Priego, E. M. Novel Colchicine-Site Binders with a Cyclohexanedione Scaffold Identified through a Ligand-Based Virtual Screening Approach. *J. Med. Chem.* **2014**, *57* (10), 3924–3938. https://doi.org/10.1021/jm401939g; b) Shchegravina, E. S.; Maleev, A. A.; Ignatov, S. K.; Gracheva, I. A.; Stein, A.; Schmalz, H. G.; Gavryushin, A. E.; Zubareva, A. A.; Svirshchevskaya, E. V.; Fedorov, A. Y. Synthesis and Biological Evaluation of Novel Non-Racemic Indole-Containing Allocolchicinoids. *Eur. J. Med. Chem.* **2017**, *141*, 51–60. https://doi.org/10.1016/j.ejmech.2017.09.055.

2. Kumar, A.; Sharma, P. R.; Mondhe, D. M., Potential anticancer role of colchicine-based derivatives: an overview. *Anticancer Drugs* **2017,** *28* (3), 250-262.

3. Key TJ, Verkasalo PK, Banks E. Epidemiology of breast cancer. Lancet Oncol. 2001;2(3):133-40.

4. Bowne-Anderson H, Hibbel A, Howard J. Regulation of Microtubule Growth and Catastrophe: Unifying Theory and Experiment. Trends Cell Biol. 2015;25(12):769-79.

5. Xiao Z, Morris-Natschke SL, Lee KH. Strategies for the Optimization of Natural Leads to Anticancer Drugs or Drug Candidates. *Med Res Rev. 2016;36(1):32-91.*

6. Gracheva IA, Shchegravina ES, Schmalz HG, Beletskaya IP, Fedorov AY. Colchicine Alkaloids and Synthetic Analogues: Current Progress and Perspectives. *J Med Chem. 2020;63(19):10618-51.*

7. Dubey KK, Kumar P, Labrou NE, Shukla P. Biotherapeutic potential and mechanisms of action of colchicine. Crit Rev Biotechnol. 2017;37(8):1038-47.

8. Tang-Wai DF, Brossi A, Arnold LD, Gros P. The nitrogen of the acetamido group of colchicine modulates P-glycoprotein-mediated multidrug resistance. Biochemistry. 1993;32(25):6470-6.

9. Li Z-H, Mori A, Kato N, Takeshita H. Synthetic Photochemistry. LVII. Facile Photochemical Construction of Hexahydro-as-indacene Skeleton, a Carbon Framework of Ikarugamycin, from High-Pressure Diels–Alder Adducts of Tropones–Cyclopentenone. *Bulletin of the Chemical Society of Japan. 1991;64(9):2778-85.*

https://doi.org/10.26434/chemrxiv-2024-rs3lh **ORCID:** https://orcid.org/0000-0003-2378-3944 Content not peer-reviewed by ChemRxiv. **License:** CC BY-NC-ND 4.0

10. Dahnke KR, Paquette LA. Exploratory Synthetic Studies Involving the Tricyclo[9.3.0.02,8] tetradecane Ring System Peculiar to the Cyathins. *J Org Chem.. 1994;59(4):885-99.*

11. Thangaraj M, Bhojgude SS, Bisht RH, Gonnade RG, Biju AT. Diels-Alder reaction of tropones with arynes: synthesis of functionalized benzobicyclo[3.2.2]nonatrienones. *J Org Chem. 2014;79(10):4757-62.*

12. Ciabattoni J, Crowley, J. E., & Kende, A. S. . Reaction of tropone with benzyne. Formation and photoisomerization of 6, 7-benzobicyclo [3.2. 2] nona-3, 6, 8-trien-2-one. Journal of the American Chemical Society. 1967;89(11):2778-9.

13. Ahmad SM, Nayak D, Mir KB, Faheem MM, Nawaz S, Yadav G, et al. Par-4 activation restrains EMT-induced chemoresistance in PDAC by attenuating MDM-2. Pancreatology. 2020;20(8):1698-710.

14. Mir KB, Faheem MM, Ahmad SM, Rasool JU, Amin T, Chakraborty S, et al. beta-(4-fluorobenzyl) Arteannuin B induced interaction of ATF-4 and C/EBPbeta mediates the transition of breast cancer cells from autophagy to senescence. Front Oncol. 2022;12:1013500.

15. Shankar S, Faheem MM, Nayak D, Wani NA, Farooq S, Koul S, et al. Cyclodipeptide c(Orn-Pro) Conjugate with 4-Ethylpiperic Acid Abrogates Cancer Cell Metastasis through Modulating MDM2. *Bioconjug Chem. 2018;29(1):164-75*.

16. Kumar A, Singh B, Mahajan G, Sharma PR, Bharate SB, Mintoo MJ, et al. A novel colchicine-based microtubule inhibitor exhibits potent antitumor activity by inducing mitochondrial mediated apoptosis in MIA PaCa-2 pancreatic cancer cells. *Tumour Biol. 2016;37(10):13121-36.*

17. Urbaniak A, Jousheghany F, Pina-Oviedo S, Yuan Y, Majcher-Uchanska U, Klejborowska G, et al. Carbamate derivatives of colchicine show potent activity towards primary acute lymphoblastic leukemia and primary breast cancer cells-in vitro and ex vivo study. *J Biochem Mol Toxicol. 2020;34(6):e22487*.

18. Lin ZY, Wu CC, Chuang YH, Chuang WL. Anti-cancer mechanisms of clinically acceptable colchicine concentrations on hepatocellular carcinoma. *Life Sci. 2013;93(8):323-8.*

19. Larocque K, Ovadje P, Djurdjevic S, Mehdi M, Green J, Pandey S. Novel analogue of colchicine induces selective pro-death autophagy and necrosis in human cancer cells. PLoS One. 2014;9(1):e87064.

20. Malumbres M, Barbacid M. Cell cycle, CDKs and cancer: a changing paradigm. Nat Rev Cancer. 2009;9(3):153-66.

21. Gabrielli B, Brooks K, Pavey S. Defective cell cycle checkpoints as targets for anti-cancer therapies. Front Pharmacol. 2012;3:9.

22. Sun Y, Liu Y, Ma X, Hu H. The Influence of Cell Cycle Regulation on Chemotherapy. Int J Mol Sci. 2021;22(13).

https://doi.org/10.26434/chemrxiv-2024-rs3lh **ORCID:** https://orcid.org/0000-0003-2378-3944 Content not peer-reviewed by ChemRxiv. **License:** CC BY-NC-ND 4.0

23. Fife CM, McCarroll JA, Kavallaris M. Movers and shakers: cell cytoskeleton in cancer metastasis. Br J Pharmacol. 2014;171(24):5507-23.

24. Choudhari AS, Mandave PC, Deshpande M, Ranjekar P, Prakash O. Phytochemicals in Cancer Treatment: From Preclinical Studies to Clinical Practice. Front Pharmacol. 2019;10:1614.

25. Chakraborty S, Kumar A, Faheem MM, Katoch A, Kumar A, Jamwal VL, et al. Vimentin activation in early apoptotic cancer cells errands survival pathways during DNA damage inducer CPT treatment in colon carcinoma model. Cell Death Dis. 2019;10(6):467.

26. Foroni C, Broggini M, Generali D, Damia G. Epithelial-mesenchymal transition and breast cancer: role, molecular mechanisms and clinical impact. Cancer Treat Rev. 2012;38(6):689-97.

27. Huber MA, Kraut N, Beug H. Molecular requirements for epithelial-mesenchymal transition during tumor progression. Curr Opin Cell Biol. 2005;17(5):548-58.

28. Busch EL, McGraw KA, Sandler RS. The potential for markers of epithelial-mesenchymal transition to improve colorectal cancer outcomes: a systematic review. Cancer Epidemiol Biomarkers Prev. 2014;23(7):1164-75.

29. Voulgari A, Pintzas A. Epithelial-mesenchymal transition in cancer metastasis: mechanisms, markers and strategies to overcome drug resistance in the clinic. *Biochim Biophys Acta. 2009;1796(2):75-90.*

30. El Hasbani G, Jawad A, Uthman I. Update on the management of colchicine resistant Familial Mediterranean Fever (FMF). Orphanet J Rare Dis. 2019;14(1):224.

31. Sardana K, Sinha S, Sachdeva S. Colchicine in Dermatology: Rediscovering an Old Drug with Novel Uses. *Indian Dermatol Online J. 2020;11(5):693-700.*

32. Banach M, Penson PE. Colchicine and Cardiovascular Outcomes: a Critical Appraisal of Recent Studies. *Curr Atheroscler Rep. 2021;23(7):32*.

33. Gigant B, Cormier A, Dorleans A, Ravelli RB, Knossow M. Microtubule-destabilizing agents: structural and mechanistic insights from the interaction of colchicine and vinblastine with tubulin. *Top Curr Chem. 2009;286:259-78*.

34. Massarotti A, Coluccia A, Silvestri R, Sorba G, Brancale A. The tubulin colchicine domain: a molecular modeling perspective. *ChemMedChem. 2012;7(1):33-42*.

35. Bhattacharyya B, Panda D, Gupta S, Banerjee M. Anti-mitotic activity of colchicine and the structural basis for its interaction with tubulin. *Med Res Rev. 2008;28(1):155-83*.

https://doi.org/10.26434/chemrxiv-2024-rs3lh **ORCID:** https://orcid.org/0000-0003-2378-3944 Content not peer-reviewed by ChemRxiv. **License:** CC BY-NC-ND 4.0

Figure Legends:

Scheme 1. Cycloaddition reaction of colchicine with benzyne precursor**.**

Scheme 2. Colchicine derivatives with different substituted benzyne precursors.

Scheme 3: HMBC Correlations of B-2a and B-2b

Table 1. IC_{50} values for the different derivatives of Colchicine screened against various cell lines.

Figure 1. Structure of Colchicine (1) and its atomic numbering (2)

Figure 1. Structural activity relationship of Colchicine

Figure 2. Cytotoxic, modulation of cell cycle regulatory proteins and apoptotic inducing potential of B-4a towards human cancer cell lines. **(A)** Structure of active compound (B-4a), **(B)** MTT assay graph showing the % inhibition in MCF-7, MDA-MB-231, MDA-MB-453, PC-3, and Hek 293 cells, treated with different concentrations of B-4a for 48h. **(C, D)** Compound B-4a mediated alterations in the cell-cycle regulatory proteins and regulation of programmed cell death in MCF-7 and MDA-MB-231 cell lines respectively. Immunoblots showing the expression of cell cycle regulatory proteins (cdk2, cdk4, cyclin D1, cyclin B1, and chk1), apoptosis markers (Bcl-2 and Bax), and β-actin as a control protein in the MCF-7 and MDA-MB-231 cells treated with B-4a. The corresponding bar graphs representing the densitometric analysis of western blots performed in ImageJ software are given in **Figure S2** respectively. Each experiment was carried out in triplicates (n=3) and results are expressed as Mean±SD, ***$p<0.001$, ns=nonsignificant.

https://doi.org/10.26434/chemrxiv-2024-rs3lh **ORCID:** https://orcid.org/0000-0003-2378-3944 Content not peer-reviewed by ChemRxiv. **License:** CC BY-NC-ND 4.0

Figure 3. Effect of compound B-4a on the tubulin polymerization in MCF-7 cells and Vimentin expression in MDA-MB-231 cells. **(A)** Representing the images of immunocytochemistry studies performed in the MCF-7 cells treated with compound B-4a, colchicine, and Flavopiridol hydrochloride for 24h. **(B)** Representing the images of immunocytochemistry studies performed to check the expression of Vimentin in the MDA-MB-231 cells treated with compound B-4a, colchicine, and Flavopiridol hydrochloride for 24h. **(C)** Histogram representing the %Mean Fluorescence of α-tubulin in MCF-7 cells. **(D)** Histogram representing the %Mean Fluorescence of Vimentin in MDA-MB-231 cells. Each experiment was carried out in triplicates (n=3) and results are expressed as Mean±SD, ***$p<0.001$, ns=nonsignificant.

Figure 4. Compound B-4a incurs….Cell cycle arrest in MCF-7 cell line. **(A, B)** PI analysis. MCF-7 cells were treated with compound B-4a, colchicine, and Flavopiridol hydrochloride for 48h and analyzed by FACS to determine the effect on the phases of the cell cycle and the corresponding bar graph shows the % total cells in the different phases of the cell cycle in the MCF-7 cells. **(C)** Images represent the nucleus stained with DAPI after post-treatment with the B-4a, colchicine, and Flavopiridol hydrochloride. Each experiment was carried out in triplicates (n=3) and results are expressed as Mean±SD, ***$p<0.001$, ns=nonsignificant.

Figure 5. (A, B) Immunoblots showing the expression of EMT-associated proteins in both MCF-7 and MDA-MB-231 cells treated with compound B-4a respectively. The corresponding bar graphs representing the densitometric analysis of western blots performed in ImageJ software are given in **Figure S3 (A)** respectively. **(C)** Gelatin matrix degradation assay. The anti-invasion effect of compound B-4a was assessed by culturing the MDA-MB-231 cells on FITC conjugated gelatin matrix. Image J software was used to analyze the threshold areas of degradation. Magnification at×10, scale bar—100 μm. **(D, E)** Wound

https://doi.org/10.26434/chemrxiv-2024-rs3lh **ORCID:** https://orcid.org/0000-0003-2378-3944 Content not peer-reviewed by ChemRxiv. **License:** CC BY-NC-ND 4.0

healing assay. MCF-7 cells treated with the B-4a, colchicine, and Flavopiridol hydrochloride and the scratched areas were photographed at zero hours and at 48h post-B-4a, colchicine, and Flavopiridol hydrochloride treatment to assess the degree of wound closure. The black outline represents the area under the wound. The corresponding bar graph shows the percent area under the wound as determined by ImageJ software. Magnification at×10, scale bar—100 μm. Each experiment was carried out in triplicates (n=3) and results are expressed as Mean±SD, ***p<0.001, ns=nonsignificant.

Figure 6. (A, B) Immunoblots showing Compound B-4a mediated modulation of cell cycle regulatory proteins, apoptotic markers, and EMT associated proteins in the cells pre and co-treated with VEGF for 24h. **(C, D)** Immunoblots showing the effect of Compound B-4a on the cell cycle regulatory proteins, apoptotic markers, and EMT associated proteins in the MCF-7 cells transiently transfected with the pCMV-cdk2 and pCMV-cdk4. The corresponding bar graphs representing the densitometric analysis of western blots performed in ImageJ software are given in **Figure S3 (B)** and **Figure S4** respectively. Each experiment was carried out in triplicates (n=3) and results are expressed as Mean±SD, ***p<0.001 ns=nonsignificant.

Figure 7. Schematic presentation of the mechanism of action of **compound B-4a** (designed by using Biorander, ChembioDraw, and Microsoft PowerPoint).

https://doi.org/10.26434/chemrxiv-2024-rs3lh **ORCID:** https://orcid.org/0000-0003-2378-3944 Content not peer-reviewed by ChemRxiv. **License:** CC BY-NC-ND 4.0